1st Advances in Solar Physics Euroconference
Advances in the Physics of Sunspots
ASP Conference Series, Vol. 118, 1997
B. Schmieder, J.C. del Toro Iniesta, M. Vázquez, eds.

First Results from EIT

F. Clette

Observatoire Royal de Belgique, B-1180 Brussels, Belgium

and the EIT Consortium :
J.-P. Delaboudinière (PI), G.E. Artzner, J. Brunaud, A.H. Gabriel, J.-F. Hochedez, F. Millier, X.Y. Song, B. Au, K.P. Dere, R.A. Howard, R. Kreplin, D.J. Michels, J.D. Moses, J.-M. Defise, C. Jamar, P. Rochus, J.-P. Chauvineau, J.-P. Marioge, R.C. Catura, J.R. Lemen, L. Shing, R.A. Stern, J.B. Gurman, W.M. Neupert, A. Maucherat, P. Cugnon, E.L. Van Dessel

Abstract. The Extreme-UV Imaging telescope has already produced more than 15000 wide-field images of the corona and transition region, on the disk and up to $1.5\,R_\odot$ above the limb, with a pixel size of $2.6''$. By using four different emission lines, it provides the global temperature distribution in the quiet corona, in the range 0.5 to 3×10^6 K. Its excellent sensitivity and wide dynamic range allow unprecedented views of low emission features, even inside coronal holes. Those so-called "quiet" regions actually display a wide range of dynamical phenomena, in particular at small spatial scales and at time scales going down to only a few seconds, as revealed by all EIT time sequences of full- or partial-field images. The initial results presented here demonstrate the importance of this wide-field imaging experiment for a good coordination between SOHO and ground-based solar telescopes, as well as for science planning.

1. Instrument Characteristics

The Extreme-ultraviolet Imaging Telescope (EIT) on the SOHO mission was designed to provide wide-field images of the corona and transition region in four different EUV emission lines (Delaboudinière et al. 1989). The EIT is specially adapted to the study of the structure and evolution of the quiet corona, in the temperature range $1-2.5 \times 10^6$ K, by providing high contrast and an unprecedented sensitivity to the weak emission of the cool and low-density plasma. The main characteristics of the instrument are summarized in Table 1 and a detailed description of the instrument can be found in Delaboudinière et al. (1995).

2. Instrument Status

Since it was put into operation, the EIT has performed according to the expectations and no major deterioration was observed in the optical components and the CCD detector. Thanks to its excellent sensitivity, exposure times below 5 s

Table 1. Main characteristics of EIT

Optics	
Mirrors	Normal-incidence multilayer-coated Zerodur
Bandpasses centers	171 Å, 195 Å, 284 Å, 304 Å
Bandpass selection	Rotatable open quadrant shutter
Effective focal length	1652 ± 2 mm
Mirror diameter	120 mm
Blocking filters	150 nm Al on Ni supporting grid
CCD detector and electronics	
Type	3-phase, MPP, back-side illuminated CCD
Array & pixel size	1024×1024 pixels ($21 \times 21\,\mu$m)
	44.7×44.7 arcmin ($2.62 \times 2.62''$)
Full well capacity	$\geq 200.000\,e^-$
Readout noise	$\simeq 50\,e^-$
Working temperature	$-68\,^\circ$C (passive cooling)
ADC resolution	14 bits ($18\,e^-$/DN)
Average telemetry rate	1 kbits/s
Data compression ratio	Rice ($\simeq 2$), Rice + ADCT ($\simeq 10$)

are sufficient to record the dimmest parts of the corona in the 171 Å and 195 Å lines, while maintaining a good time resolution. Full-field full-resolution images, acquired as part of the EIT synoptic program, can be transmitted to ground in about 20 minutes. However, sequences of subimages can be made at much higher cadences, up to 12 frames/min in the early phase of the mission and even to 1 image/s in the near future. An increase of the telemetry rate from 1 kbits/s to 2.7 or 4.4 kbits/s is currently planned, in a permanent effort to maximize the output of the experiment.

Large efforts are also dedicated to the correction of spatial nonuniformities in the instrument response. These are produced by several effects :

- a grid pattern produced by the focal aluminium filter (blocking prefilter deposited on a nickel grid). This 30 % modulation is now successfully extracted from the in-flight images themselves.
- the CCD flat-field (magnitude of the defects : 6 % rms).
- the vignetting function (maximum attenuation : 6.5 %).
- a light leak in the focal aluminium filter (pinhole).
- a negative "burn-in" image of the Sun, due to an accidental malfunction of the mechanical shutter that happened in July 96.

The last two effects appeared during the mission, and must be diagnosed entirely from the in-flight images. Moreover, all the above components, except vignetting, evolve with time, so the flat-field correction is now monitored and updated on a regular basis, in order to maintain an accuracy close to 1 % for each separate correction.

3. EIT Synoptic Images : a Global View

The overall aspect of the Sun is changing rapidly as a function of temperature. In the Fe IX–X lines (171 Å) formed at 1×10^6 K, an ubiquitous diffuse background covers the low corona, and significant emission is detected even inside the coronal holes. As we go up in temperature to 1.5×10^6 K (Fig. 1), in Fe XII line (195 Å), bright points are scattered across the quiet surface, and also inside coronal holes. This is the EIT bandpass providing the highest contrast between coronal holes and the rest of the corona. Near their footpoints, most polar plumes appear as cylindrical tubes substended by a bright point at their base.

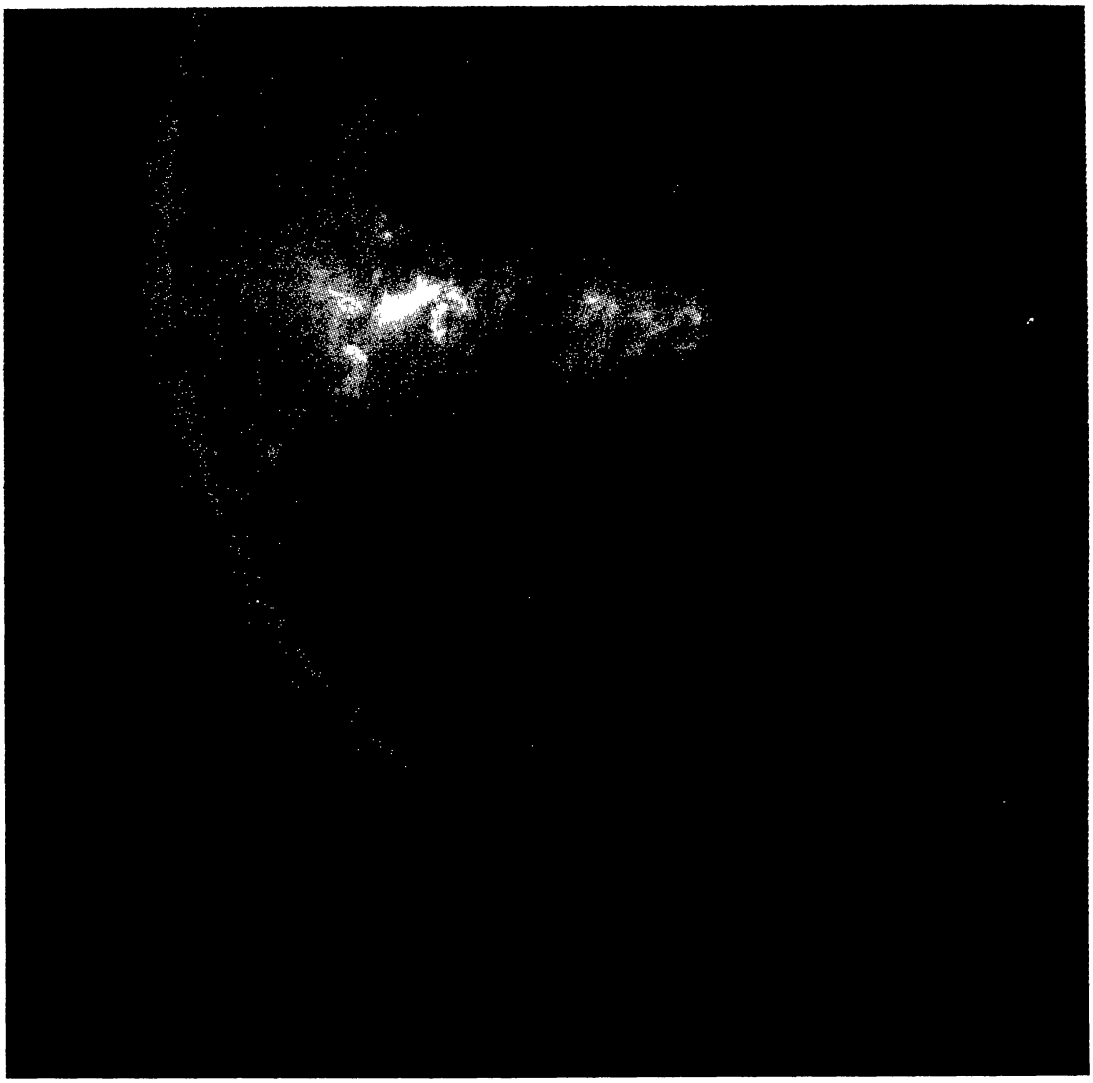

Figure 1. Enlarged portion of a sample full-field synoptic image acquired on May 10, 1996 at $5^h\,46^m\,44^s$ UT and showing the solar corona at a temperature of 1.5×10^6 K (Fe XII line; Exposure : 4.0 s).

At 2 million degrees, in the Fe XV line (284 Å), the diffuse emission of the quiet regions becomes much weaker and strong emission is now concentrated

in compact loop systems. Most of those loops are hot at the top, with cooler footpoints, and are recorded over their full length only in these Fe XV images. This view becomes similar to images from the SXT experiment on YOHKOH, at the lowest plasma temperatures accessible to that instrument (Hara et al. 1992).

Besides the coronal lines, EIT also provides global views of the transition region at 10^5 K in the He II line (304 Å). The quiet disk is dominated by the chromospheric network, but the most striking features appear on the limb. The polar holes are populated by macrospicules, which are almost absent in other parts of the solar surface. Some of these short-lived features can reach an altitude of 10^5 km above the surface. In this phase of low solar activity, there are many polar crown filaments concentrated at mid- and high-latitude, that can be seen as absorption features in the coronal lines. Filaments often mark the base of large dark cavities and arcades observed above the limb at coronal temperatures.

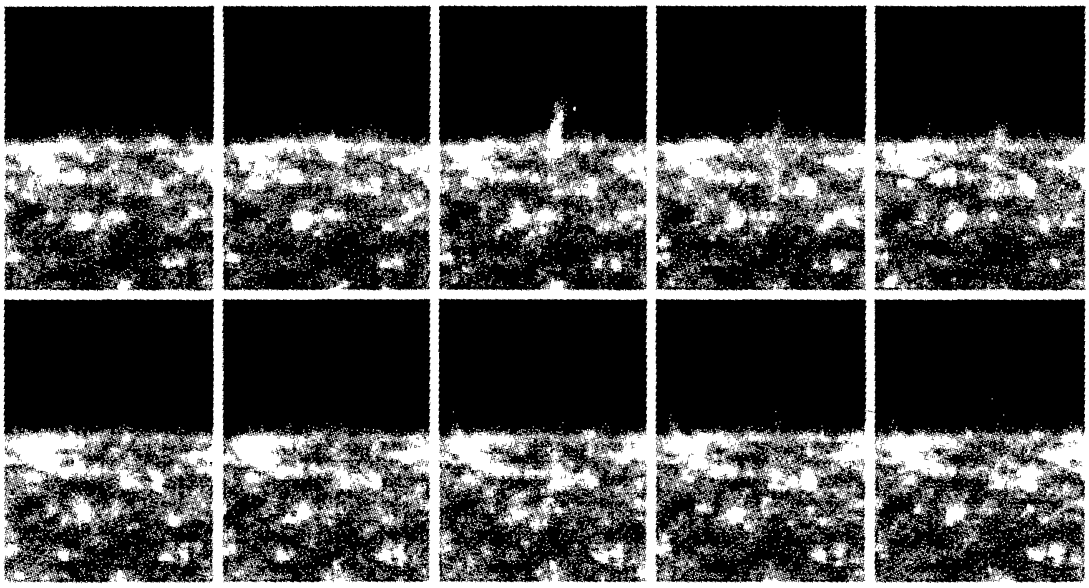

Figure 2. Image sequence taken on September 6, 1996 and showing the eruption of a large macrospicule in the North polar hole (Time interval : $15^h\,31^m$ – $16^h\,11^m$ UT; time step : 5 min). An initial surge is followed by the fast rise of a narrow jet (width $\simeq$ 5000 km; speed $\simeq$ 150 km/s) which finally falls back to the surface.

4. Dynamical Behaviour of the Quiet Sun

Diverse manifestations of small-scale solar activity are revealed in detail for the first time by time lapse movies built from EIT image sequences. In the transition region, macrospicules are erupting continuously in the polar regions, with typical lifetimes of only a few minutes (Fig. 2). Most filaments are also short-lived, with lifetimes shorter than one day. and many eruptive prominences have already been captured in action by EIT, despite the very low level of activity.

In the corona, the quiet coronal background is made of an intricate pattern of a loop-like structures, which are continuously transforming and experiencing small-amplitude brightness changes over timescales ranging from minutes to hours. Inside coronal holes, EIT images show numerous examples of plume formation simultaneously with the sudden emergence of bright points, and hint that a close physical connection exists between both objects. Finally, in parallel with SXT on the YOHKOH mission, EIT can also bring a complementary view of the dynamics of minor activity inside active regions. For instance, the brightness changes of individual loops observed at the relatively low temperatures of $1-2 \times 10^6$ K are reminiscent of the transient brightenings discovered in SXT images (Shimizu et al. 1992). Thanks to its high time resolution, EIT shows that, in compact loops, such random brightenings can happen over intervals of only a few seconds.

It is important to note that such small-scale activity can be found in any EIT image sequence at any place on the Sun. This new class of activity, uncovered by EIT, is thus likely to bring a significant additional contribution to the global energy deposition in the corona. One of our main scientific objectives is now to quantify this new contribution.

5. Conclusion

In the first six months of the mission, EIT has already produced more than 15000 images, including about 3000 synoptic images. This constitutes an homogeneous data set amounting to nearly 10 GBytes. Such images provide an ideal tool for the coordination of observations in space and on the ground. The wide field of EIT provides the global context, as well as a basic temperature diagnostic over the whole visible face of the Sun. It can also produce image sequences when other instruments do not offer enough time resolution. Given these unique capabilities and the abundance of data, all solar physicists are encouraged to submit observing programs, or simply to contribute to the analysis of this rich harvest of solar EUV images.

Proposals from countries in Europe should be addressed to : Dr. Pierre Cugnon, Observatoire Royal de Belgique, Avenue Circulaire, 3, B–1180 Bruxelles, Belgium. E-mail : pierrec@oma.be. More information can be found on Internet at : http://umbra.gsfc.nasa.gov/eit

References

Delaboudinière et al. 1989, ESA SP – 1104, 43.

Delaboudinière et al. 1995, Solar Phys., 162, 291.

Hara, H., Tsuneta, S., Lemen, J.R., Acton, L.W. & McTiernan, J.M. 1992, PASJ, 44, L135.

Shimizu, T., Tsuneta, S., Acton, L.W., Lemen, J.R. & Uchida, Y. 1992, PASJ, 44, L147.